# 4.4 WARM SEASON LIGHTNING PROBABILITY PREDICTION FOR CANADA AND THE NORTHERN UNITED STATES

William R. Burrows*
Meteorological Service of Canada, Edmonton, Alberta
Colin Price
Tel Aviv University, Tel Aviv, Israel
Lawrence Wilson
Meteorological Service of Canada, Dorval, Quebec

## 1. INTRODUCTION

The North American Lightning Detection Network (NALDN) provides continuous lightning detection over the contiguous United States and over Canada to about 65°N in the northwest and 55°N in the northeast since February 1998. Locations of detectors in the network are shown in Orville et al. (2002). Detection efficiency over this area is 80-90+% (Cummins et al., 1998). The Meteorological Service of Canada (MSC) receives lightning flash reports for Canada and the northern United States to 35°N east of 100°W and to 40°N west of 100°W. 1998-2000 lightning climatology for this region was established by Burrows et al. (2002), and Orville et al. (2002). Complex patterns of lightning occurrence were revealed, showing strong latitudinal, seasonal, and diurnal dependencies, and significant influences by topography and land-water boundaries.

Canada is a vast country. Little or no information about lightning occurrence was previously available over much of its area. Lightning is not directly predicted by operational weather prediction models. There is a need for improved thunderstorm prediction guidance for public and aviation forecasts. A starting point for this is statistical models which relate observed lightning to predictors known to represent favourable conditions for lightning occurrence.

We built models with any predictors known or thought to be related to lightning through convection, moisture, lift, and climate controls. As this was our first attempt at building statistical lightning prediction models, many candidate predictors were used in order to determine which would be necessary for inclusion in future models. Models valid for each month May to September were developed to predict the probability of lightning occurrence in each of the three-hour intervals in a twenty-four hour period using pooled learning data from 2000 and 2001. Dynamic predictors were derived from output of the GEM weather prediction model (Coté et al., 1997) at the Canadian Meteorological Center (CMC). Models were built for 5º latitude by 5º longitude sectors using tree-structured regression with data from 2000 and 2001, and run in real time in 2003. Only sketchy details are given here due to space limitation. A paper has been submitted to Weather and Forecasting.

* Corresponding author address: William R. Burrows, Environment Canada - MSC/PNR - Science Division, Twin Atria Building, 4999 - 98 Avenue, Room 200, Edmonton, Alberta, T6B 2X3; e-mail: william.burrows@ec.gc.ca

## 2. PREDICTAND, PREDICTORS, METHODS

Flash reports in each of the 8 three-hour time segments per 24-hour diurnal period were transformed to a grid of approximately 22 km resolution, which is the resolution of the GEM model. Each report was assigned a weight of 1 when 0 to 10 km from a grid point, decreasing linearly to 0 at 20 km. We refer to the gridded predictand as flash report density (FRD). Cloud-to-ground flashes were not separated from cloud-to-cloud flashes since we wished to predict any lightning activity. Only about 4% of lightning detected by the NALDN is cloud-cloud.

During this study we found that a range of FRD was often seen in events with similar predictor values, and that significantly more variance reduction could be achieved by linearizing the predictand. FRD was transformed into 11 categories of flashes per three hours: (1) 0-.01, (2) >.01-.50, (3) >.50-1.0, (4) >1.0-2.7, (5) >2.7-7.4, (6) >7.4-20, (7) >20-55, (8) >55-148, (9) >148-403, (10) >403-1097, (11) >1097-2981. The boundaries of categories 4-11 are the successive values of $e^1$ to $e^8$ (higher values rounded to the nearest integer). The transformed FRD data were then treated as a continuous distribution for building models.

The predictand was matched with several candidate predictors known or thought to be associated with lightning through moisture, convection, lift, and climate controls. For dynamic predictors the mean, maximum (minimum where appropriate), and change in three-hour time segments were used. Thus three separate predictors were derived from a basic predictor such as the (500-1000) hPa layer thickness. Several are closely related or redundant. This is not problematical for the tree-structured regression algorithm used. GEM model output archived in 6-hour intervals for 2000 and 2001 were linearly interpolated to intermediate 3-hour times before predictor calculation. Like most models, GEM suffers from spin-up error for the first few forecast hours. To circumvent this, 00-hour forecast data was replaced with the 12-hour forecast from the previous run. Thus at both 0000 UTC and 1200 UTC all predictors for 0-3 hour and 3-6 hour periods are calculated with data interpolated from the previous run's 12-hr forecast and the current run's 6-hr forecast, while predictors for 6-9 hour and 9-12 hour periods are

calculated with data from the current run's 6-hour and 12-hour forecasts. Forecast precipitation was not used because only 6-hour accumulations were available.

Due to the large geographical area, data were stratified into eighty-two 5º lat by 5º lon sectors. Separate models were built for each sector for each month May to September. Predictors were matched with the transformed FRD predictand at every grid point for each three hour period. This gave a total of eight training data sets per 24 hours (four for the 12-hour period from 0000 UTC and four for the 12-hour period from 1200 UTC), for a total of 3280 data sets.

After random permutation of cases in each FRD category, 70% of the learning data set in each category was reserved for training and 30% for validation. Statistical models were derived by tree-structured regression (Brieman et al., 1984). This is a non-linear, non-parametric algorithm that minimizes residual variance of the predictand by finding a series of decisions that use predictor threshold values to cluster groups of similar training data into "terminal nodes". Starting at the root node, training data is separated into left and right child nodes by searching through all values of all predictors until a threshold value is found that gives the minimum residual predictand variance after the split. Further partitioning of child nodes continues along each tree branch until further reduction of variance cannot be achieved or a user-determined limit on node population is reached, a limit we set at 25 cases. If necessary, the tree is then "pruned upwards" along its branches until a tree structure is found that fits the validation predictand data with least error. Terminal nodes are distinct from each other, thus the fitted predictand is piecewise-continuous. The prediction value assigned to each terminal node is usually the mean of the predictand calculated from the case population in the node. A probability distribution for predictand categories can be established for each terminal node from the distribution of predictand values in the learning data cases that clustered into it. For example, if a terminal node contains 500 cases, 25 of which were FRD category 1 (no lightning), 475 of which were category 2-11, and 100 of those which were category 7-11, then for meteorological situations which reach this node the predicted probability of no lightning is .05, of lightning is .95, and of frequent lightning is .2.

Error reduction achieved by most of the tree-structured statistical models was in the range .4 to .7 of initial predictand variance. Decision trees were least complicated in northern latitudes and most complicated in southern latitudes, where there were several hundred terminal nodes in all trees.

Predictors were ranked overall by adding predictor ranks in decision trees for all months, times, and 5º lat by 5º lon sectors, and scaling the result to a scale of 0 to 100. Overall, the highest-ranked predictors are Showalter index, mean sea level pressure, and troposphere precipitable water. The lifted index ranks higher than the Showalter index in the far west and the north but not elsewhere. Other highly ranked predictors overall are the SWEAT index, layer thickness (usually (500-1000) hPa), depth of cloud above the height of 0º C, upper troposphere precipitable water, potential cloud top height, tropopause temperature, and 500 hPa geopotential height. In the north the Price and Rind function (Price and Rind, 1992) was among the ten highest-ranked predictors for lightning. The three-hour average of a basic predictor was far more important than its maximum or minimum value, consistent with the derivation of the predictand from three-hour total lightning flash report density. Three-hour changes of 500 hPa geopotential height, thickness, and mean sea level pressure were highly ranked predictors in many areas, likely since they are representative of frontal motion in temperate latitudes. CAPE is not included among the ten highest-ranked predictors in any region but was assigned a middle ranking overall. Thus, while CAPE is an essential ingredient for generation of convection, other characteristics of the environment such as potential for lift determine whether convection will proceed to an extent to cause lightning.

## 3. RESULTS, DISCUSSION, CONCLUSIONS

Predictions for the probability of lightning were run at CMC in real time May-September 2003. Forecasts were made in three-hour intervals for 00-hr to 48-hr projection times for 0000 UTC GEM runs, and 00-hr to 24-hr projection times for 1200 UTC runs. Figure 1 shows the 21-24 hour lightning probability forecast valid 0000 UTC 28 June 2003. Probability ranges are color coded in 10 percent ranges. Areas where no forecast model was available are shown as dark blue. The color bar shows this color representing the range < 0 to -10 percent. It also shows a 100-110 percent range, but the true values are all 100 percent.

The probability forecasts were verified by taking the group of forecast-observation pairs in a 100 km radius ρ around each grid point. Lightning was deemed to have occurred if it was observed for any member of the group. Three forecasts were defined from the forecasts in a group: (1) the max forecast probability ( $f_{\max}$ ), (2) the mean forecasts probability ( $f_{mean}$ ), and (3) a hybrid forecast defined as

$$\Phi^{p}_{month} < \Phi^{p}_{thresh} : \quad f_{hybrid} = f_{mean}$$

$$\Phi^{p}_{month} \geq \Phi^{p}_{thresh} :$$

$$.4 \leq f_{\max} \leq .6, \quad f_{hybrid} = \frac{f_{mean} + f_{\max}}{2}$$

$$f_{\max} > .6, \quad f_{hybrid} = f_{mean} \qquad (1)$$

where where $\Phi^{p}_{month}$ is a monthly "climate frequency" (fraction of grid points over a month where lightning was observed anywhere within ρ in a three-hour diurnal period *p*), and $\Phi^{p}_{thresh}$ is a threshold monthly climate frequency set at .105. Figure 2 shows ROC and reliability curves for hybrid forecasts for all 21-24 forecasts issued at 0000 UTC for July for the region east of 100°W in Fig.1. The area under the ROC curve ( $A_{ROC}$ ) is a respectable .805, giving a ROC skill score

(Kharin and Zwiers, 2002) $S_{ROC}$ =.61. The reliability curve runs very close to the diagonal for the forecast probability range .2 to .8, and not far away for the remaining ranges, showing good forecast reliability.

Figure 3 shows monthly $A_{ROC}$ values for May, June, July, and September 2003 for all projection times. August was not verified since September models were inadvertently used for August forecasts. Figure 3 shows monthly $A_{ROC}$ values for $f_{hybrid}$ for all projection time segments 0-3 hours to 45-48 hours. As would be expected, $A_{ROC}$ values show a declining trend as projection time increases. $A_{ROC}$ values are well above .75 ($S_{ROC}$ =.5) at all projection times except 36-42 hours in some months, although they are still above .70 ($S_{ROC}$ =.4). In most months there is evidence of a diurnal trend in $A_{ROC}$ values and a tendency to spike lower at times of minimal lightning activity (usually somewhere in the valid period 09-18 UTC). This may be NWP model-related, as there may be a diurnal variation in the ability of the GEM model to resolve the boundary layer.

We conclude that these models predict the probability of lightning occurrence in three-hour projection time intervals from 0-3 hours to 45-48 hours with good accuracy, at least for public forecasts. Preliminary results for summer 2004 show prediction accuracy was relatively good, even though a new GEM model was introduced in May.

## 4. REFERENCES


Brieman, L., Friedman, J. H., Olshen, R. A., and Stone, C. J., 1984: *Classification and Regression Trees*. New York: Chapman & Hall / CRC Press. (Formerly Monterrey: Wadsworth and Brooks/Cole).

Burrows, W. R., P. King, P. J. Lewis, B. Kochtubajda, B. Snyder, and V. Turcotte, 2002: Lightning occurrence patterns over Canada and adjacent United States from lightning detection network observations. *Atmos.-Ocean,* **40**, 59-80.

Burrows, W. R., C. Price, and L. J. Wilson, 2004: Warm season lightning probability prediction for Canada and the northern United States, *Wea. Forecasting*, (submitted 29 June 2004).

Côté, J., S. Gravel, A. Méthot, A. Patoine, M. Roch, and A. Staniforth, 1997: The operational CMC/MRB Global Environmental Multiscale (GEM) model: Part I - Design considerations and formulation, *Mon. Wea. Rev.*, **126**, 1373-1395.

Cummins, K. L., M. J. Murphy, E. A. Bardo, W. L. Hiscox, R. B. Pyle, and A. E. Pifer, 1998: A combined TOA/MDF technology upgrade of the U.S. National Lightning Detection Network. *J. Geophys. Res.,* **103 (D8),** 9035-9044.

Kharin, V. V., and F. W. Zwiers, 2003: On the ROC score of probability forecasts. *J. Climate*, **16**, 4145-4150.


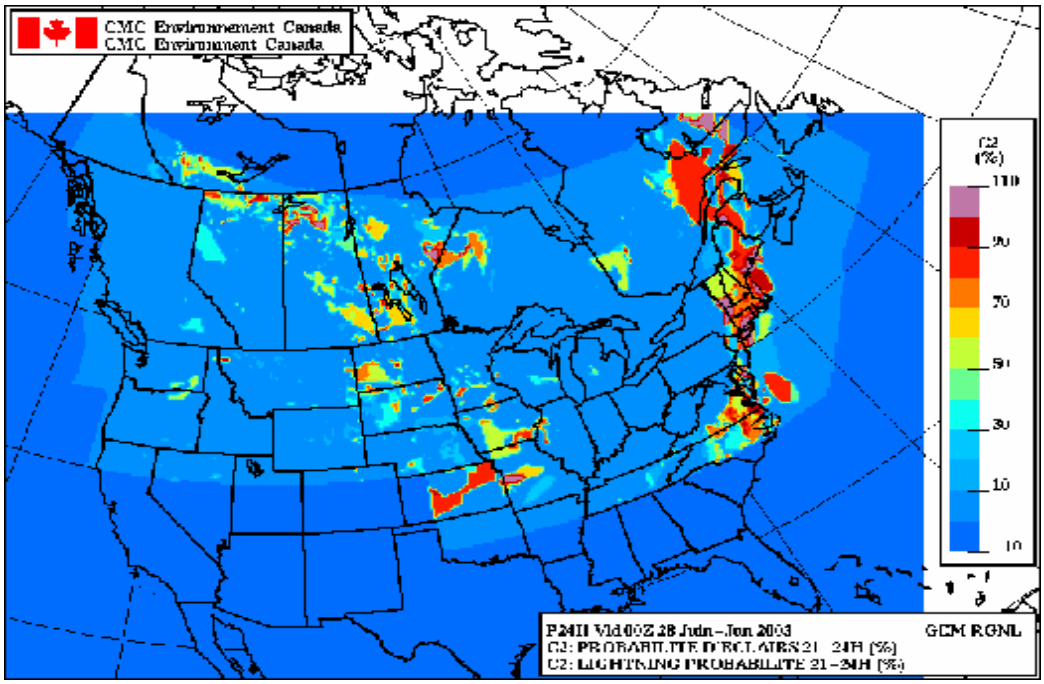


Figure 1. 21-24 hour forecast of the probability of lightning, valid 2100 UTC 27 June to 0000 UTC 28 June 2003.

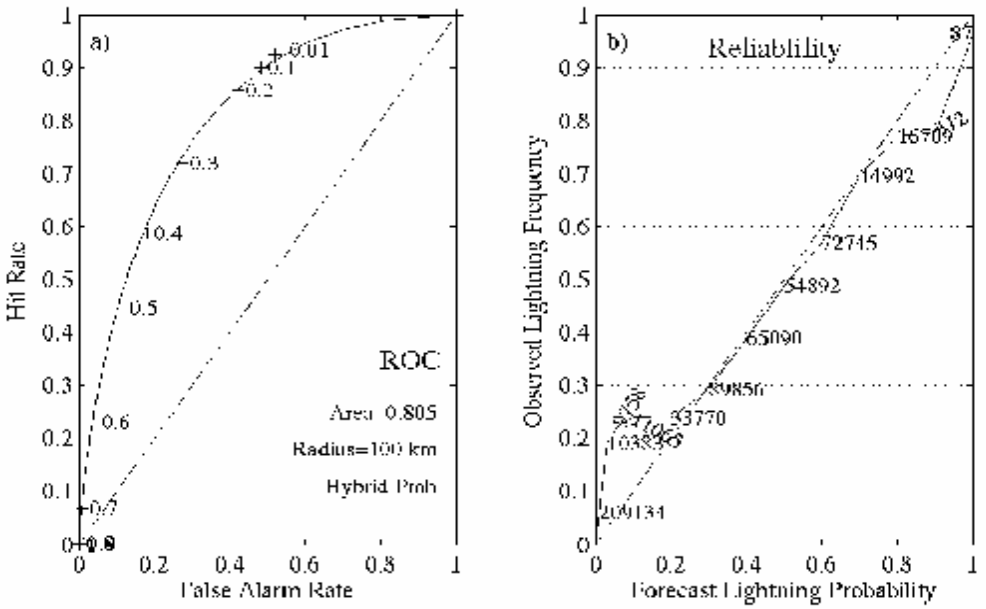


Figure 2. ROC and reliability curves for all forecasts issued at 0000 UTC for the 21-24 hour projection time for July 2003, for the east region east fo 100W in Fig1. Curves shown are for $f_{hybrid}$ forecasts defined by (1).

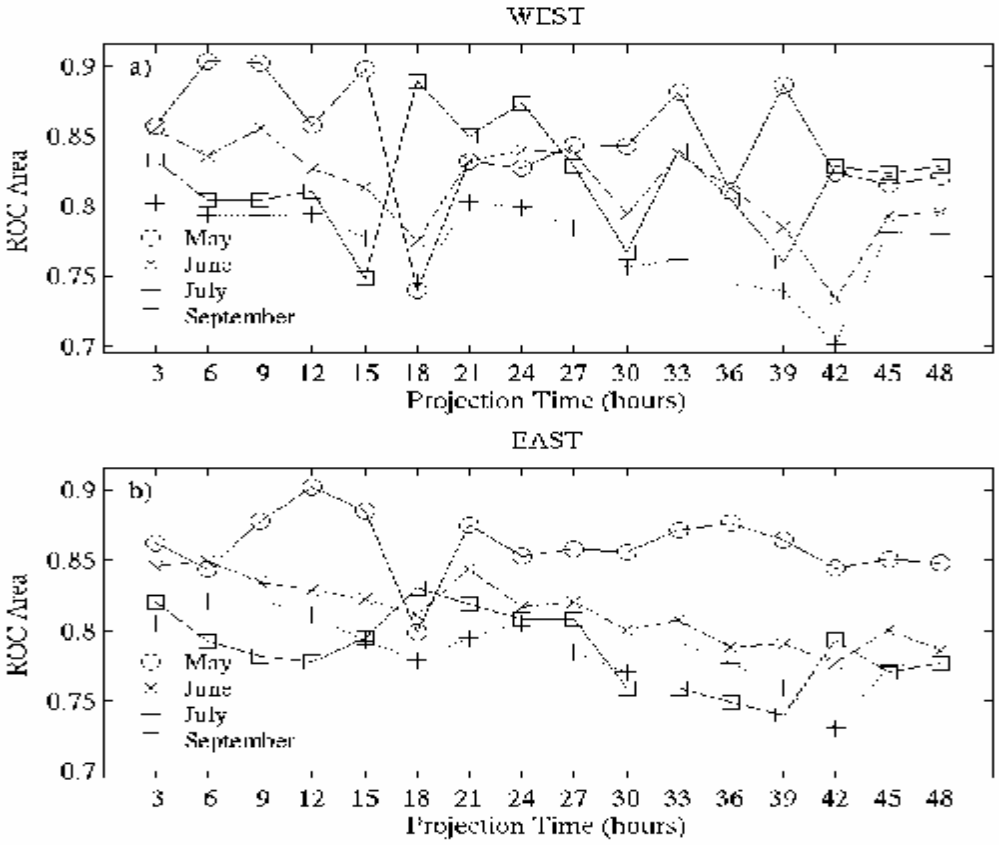


Figure 3. Monthly $A_{ROC}$ values for $f_{hybrid}$ forecasts, for projection times in 3-hr time segments ending in hour shown on abscissa.